Overexpression of miR-361-5p plays an oncogenic role in human lung adenocarcinoma through the regulation of *SMAD2*

NORAHAYU OTHMAN[1] and NOOR HASIMA NAGOOR[1,2]

[1]Institute of Biological Sciences (Genetics and Molecular Biology), Faculty of Science, and
[2]Centre for Research in Biotechnology for Agriculture (CEBAR), University of Malaya,
Lembah Pantai, 50603 Kuala Lumpur, Malaysia

Abstract. The silencing of *Bcl-xL* in the non-small cell lung cancer (NSCLC) cell line, A549, downregulates miR-361-5p expression. This study aimed to determine the biological effects of miR-361-5p on NSCLC, and to elucidate the molecular mechanisms through which apoptosis is regulated. MicroRNA (miRNA or miR) functional analyses were performed via transfection of miR-361-5p mimics and inhibitors, demonstrating that the inhibition of miR-361-5p induced the apoptosis of NSCLC cells. To elucidate the function of miR-361-5p *in vivo*, cells transfected with miR-361-5p inhibitors were microinjected into zebrafish embryos, and immunostained using antibodies to detect the active form of caspase-3. Co-transfection with si*Bcl-xL* and miR-361-5p mimics illustrated the association between *Bcl-xL*, miR-361-5p and apoptosis; miR-361-5p mimics blocked the apoptosis initiated by si*Bcl-xL*. Luciferase reporter assays identified mothers against decapentaplegic homolog 2 (*SMAD2*) as a novel target of miR-361-5p and the reduction of its protein level was validated by western blot analysis. To confirm the molecular mechanisms through which apoptosis is regulated, gene rescue experiments revealed that the ectopic expression of *SMAD2* attenuated the inhibitory effects on apoptosis induced by miR-361-5p. In this study, to the best of our knowledge, we provide the first evidence that miR-361-5p functions as an oncomiR in A549 and SK-LU-1 cells through the regulation of *SMAD2*, suggesting that miR-361-5p may be employed as a potential therapeutic target for the miRNA-based therapy of NSCLC.

Correspondence to: Professor Noor Hasima Nagoor, Institute of Biological Sciences (Genetics and Molecular Biology), Faculty of Science, University of Malaya, Lembah Pantai, 50603 Kuala Lumpur, Malaysia
E-mail: hasima@um.edu.my

Introduction

Lung cancer remains the most common type of cancer worldwide with an estimated 1.8 million new cases in 2012 (12.9% of the total cancer cases) and accounting for 23.6% of total deaths (1). While treatment for lung cancer is available in the form of surgical resection, chemotherapy and radiation, the 5-year survival rate remains very low at only 16.6% (2,3). It is therefore important to gain a better understanding of the molecular mechanisms that are involved in lung carcinogenesis with the aim to identify diagnostic and prognostic markers for the early detection and a more targeted treatment of lung cancer.

Apoptosis plays an important role during development and in the maintenance of multicellular organisms through the removal of damaged, aged or autoimmune cells (4). Studies conducted on non-small cell lung cancer (NSCLC), which accounts for the majority of lung cancer cases (5), have demonstrated that the expression of B-cell lymphocyte xL (*Bcl-xL*), the other major prototype of the anti-apoptotic *Bcl-2* gene, is elevated in NSCLC, leading to the inhibition of apoptosis and a poor prognosis (6). A previous study conducted by our group demonstrated that the silencing of *Bcl-xL* induced alterations in microRNA (miRNA or miR) expression in the A549 lung adenocarcinoma cell line, and the rippling effects of the alteration in miRNA expression towards target genes may contribute to the induction of apoptosis. miR-361-5p was one of the miRNAs found to be significantly downregulated following *Bcl-xL* silencing (7).

miRNAs are non-coding RNAs of approximately 19 to 23 nucleotides in length, which post-transcriptionally regulate gene expression (8). These regulatory elements play a role in a wide range of biological processes, including cell proliferation (9), differentiation (10), drug sensitivity (11) and apoptosis (12). A number of studies carried out in recent years have aimed at elucidating the specific miRNAs associated with apoptosis in cancer and their related target genes (13-17).

In this study, we aimed to determine whether miR-361-5p, which was downregulated in response to *Bcl-xL* silencing, as shown in our previous study (7), is involved in the regulation of

the apoptosis of NSCLC cells and to investigate the molecular mechanisms that mediate these effects.

Materials and methods

Cell lines and culture conditions. The human lung adeno-carcinoma cell lines, A549 (Cancer Research Malaysia, Subang Jaya Medical Centre, Subang Jaya, Selangor Malaysia) and SK-LU-1 (AseaCyte Pte. Ltd., Subang Jaya, Selangor, Malaysia), were maintained in RPMI-1640 (HyClone/GE Healthcare Life Sciences, Pittsburgh, PA, USA) and MEM-α (Gibco/Thermo Fisher Scientific, Waltham, MA, USA), respectively, containing 10% (v/v) fetal bovine serum (FBS) (HyClone/GE Healthcare Life Sciences), and maintained in 5.0% CO_2 levels at 37.0°C in a humidified atmosphere.

Transfection with miRNA mimic and inhibitors. The cells were seeded 24 h prior to transfection with 80.0 nM miRIDIAN microRNA human miR-361-5p mimics or hairpin inhibitors (GE Healthcare Dharmacon, Lafayette, CO, USA) using the DharmaFECT transfection reagent (GE Healthcare Dharmacon), as per the manufacturer's instructions. miRIDIAN microRNA Mimic Negative Control #1 and miRIDIAN microRNA Hairpin Inhibitor Negative Control #1 (GE Healthcare Dharmacon) were used as negative controls.

Combined transfection of siBcl-xL and miR-361-5p. The cells were plated 24 h prior to transfection with 100.0 nM Stealth RNAi (si*Bcl-xL*) using Lipofectamine 2000 reagent (Invitrogen, Carlsbad, CA, USA), as per the manufacturer's instructions. At 24 h post-transfection, the spent media were removed and the cells were transfected with miR-361-5p mimics or mimic negative control (NC).

Annexin V-FITC apoptosis assay. Apoptosis was detected using the FITC Annexin V apoptosis detection kit (BD Biosciences, Franklin Lakes, NJ, USA) at 72 h post-transfection, as per the manufacturer's instructions. Apoptosis was detected in 1.0×10^4 cells using the BD FACSCanto™ II flow cytometer (BD Biosciences) and analyzed using BD FACSDiva™ software (BD Biosciences).

Caspase-3/7 activity assay. Caspase-3 and -7 activities were determined using the Caspase-Glo 3/7 assay kit (Promega, Madison, WI, USA), at 48 h post-transfection, as per the manufacturer's instructions. Luminescence was detected using the GloMax Multi Luminescence Multimode Reader (Promega).

Zebrafish care and use. Experiments involving zebrafish were approved by the University of Malaya, Faculty of Medicine, Institutional Care of Use Committee (FOM IACUC) (Ethics reference no. 2015-181006/IBS/R/NO) and complied with all relevant animal welfare laws, guidelines and policies. Wild-type *Danio rerio* zebrafish embryos were cared for and maintained using standard husbandry practices.

Zebrafish microinjection. Approximately 150 zebrafish embryos (Zebrafish Laboratory, Department of Biomedical Science, Faculty of Medicine, University of Malaya, Kuala Lumpur, Malaysia) were injected with A549 cells transfected with 80.0 nm miR-361-5p inhibitors or their corresponding negative controls. The A549 cells re-suspended in serum-free RPMI were injected at the superficial location of the yolk near to the perivitelline space of the embryos using a FemtoJet Microinjector (Eppendorf, Hamburg, Germany) and InjectMan NI 2 Micromanipulator (Eppendorf) with constant injection pressure and injection time. The injection volume and cell suspension was calibrated to be approximately 100-200 cells/injection in each embryo. Following microinjection, the embryos were immediately incubated at 37°C overnight.

Whole mount caspase-3 immunofluorescence. At 12 h post-injection, the embryos were fixed in 4% paraformalde-hyde overnight at 4°C, and then dehydrated in methanol for 2 h at -20°C. Following rehydration, the embryos were washed several times with 1% DMSO, 0.1% Triton in PBS (1X PDT) and blocked for 1 h at 25°C with gentle shaking in 10% FBS, 2% BSA in PBST (blocking buffer). The embryos were then stained with purified rabbit anti-active caspase-3 antibody (Cat. no. 559565, BD Biosciences) (1:500 dilution) for 2 h at 25°C followed by washes in PDT. The embryos were again blocked with blocking buffer, and then stained with anti-rabbit IgG Fab2 Alexa Fluor 647 Conjugate (Cat. no. 4414S, Cell Signaling Technology, Danvers, MA, USA) (1:500 dilution) overnight at 4°C. The following day, the embryos were washed with PDT prior to visualization and imaging using a Leica confocal laser-scanning microscope SPII and Leica Application Suite (LAS) software v5.0 (Leica, Wetzlar, Germany). Fluorescence was quantified using ImageJ Analyst [National Institutes of Health (NIH), Bethesda, MD, USA] software. The threshold was set to eliminate background fluorescence and embryos were analyzed to generate arbitrary fluorescence units.

Bioinformatics analyses of miRNA gene targets. The putative miRNA targets were identified using TargetScan Human v5.2, a database of conserved 3'UTR targets, found at http://www.targetscan.org/ (Whitehead Institute for Biomedical Research, Cambridge, MA, USA). TargetScan allows for the ranking of predicted miRNA targets based upon a total context+ score, which is the sum of the contribution of six targeting factors which include site type, site number, site location, local AU content, 3'-supplementary pairing, target site abundance, and seed-pairing stability. The total context+ score indicates the relative repression of mRNA, with low context scores being more favorable (18). Gene-annotation enrichment analyses of the predicted miRNA targets with total context+ scores of <0 were then performed using the web tool made up of an integrated biological knowledgebase and analytic tools (19) called Database for Annotation, Visualization and Integrated Discovery (DAVID) v6.7 at http://david.abcc.ncifcrf.gov/summary.jsp (SAIC Frederick, Inc. Frederick, MD, USA) using default parameters. Data from TargetScan 5.2 and DAVID were combined to generate a hypothetical pathway of the association between miR-361-5p and its gene targets.

Dual luciferase reporter assay system. The cells were plated 24 h prior to co-transfection with 40.0 ng of 3'UTR reporter constructs containing wild-type or mutated bindings sites

and 80.0 nM of miR-361-5p mimic/hairpin inhibitor or mimic NC/hairpin inhibitor NC using DharmaFECT transfection reagent. Relative luciferase activity was assayed at 48 h post-transfection using the Dual Luciferase Reporter Assay System (Promega) and detected on the GloMax Multi Luminescence Multimode Reader (Promega). Luciferase activity was normalized to the internal control *Renilla* activity in each well.

Protein extraction and western blot analysis. Proteins were extracted at 48 h post-transfection using the NE-PER® Nuclear and Cytoplasmic Extraction kit (Thermo Fisher Scientific), as per the manufacturer's instructions. Size separation by electrophoresis in 12.0% (w/v) SDS-PAGE was performed prior to transfer to nitrocellulose membranes. The membranes were blocked with 5% (w/v) non-fat skimmed milk for 1 h at 25°C and incubated overnight at 4°C with primary monoclonal rabbit antibodies: Mothers against decapentaplegic homolog 2 (SMAD2) (Cat. no. 3122, Cell Signaling Technology) (1:1,000 dilution) and GAPDH (Cat. no. 2188, Cell Signaling Technology) (1:10,000 dilution). The membranes were subsequently washed and incubated with secondary goat anti-rabbit IgG HRP-linked antibody (Cat. no. 7074, Cell Signaling Technology) (1:1,000 dilution) and anti-biotin HRP-linked antibody (Cat. no. 7075, Cell Signaling Technology) (1:1,000 dilution). Bands were visualized using Western Bright Quantum (Advansta, Menlo Park, CA, USA) on the Fusion FX7 system (Vilber Lourmat, Eberhardzell, Germany) and quantified using ImageJ Analyst software with band intensities normalized to GAPDH.

Gene rescue experiments. The cells were plated 24 h prior to transfection with 80.0 nM miR-361-5p mimics or mimic NC. At 6 h post-transfection, the spent media were removed and the cells transfected with 50.0 ng of plasmid expressing the SMAD2 gene without its 3'UTR (pCMV6/SMAD2) (OriGene Technologies, Rockville, MD, USA). Empty pCMV6 (OriGene Technologies) was used as a control. The protein levels of SMAD2 were determined 48 h post-transfection by western blot analysis, while apoptosis was detected using the FITC Annexin V apoptosis detection kit and Caspase-Glo 3/7 assay kit as described above.

Statistical analysis. All *in vitro* experiments were performed in triplicate independent experiments and presented as the means ± standard deviation (SD). *In vivo* experiments were performed with sample size of 15 zebrafish embryos per treatment group. An unpaired Student's t-test was used to determine the statistical significance of the differences between 2 groups of data, where a P-value ≤0.05 was considered to indicate a statistically significant difference. The analysis of statistical significance between 3 or more groups of data was performed using one-way analysis of variance (ANOVA), followed by Dunnett's Multiple Comparison post-hoc test where a P-value <0.05 was considered to indicate a statistically significant difference.

Results

Suppression of miR-361-5p expression promotes the apoptosis and induces cell cycle arrest of A549 and SK-LU-1
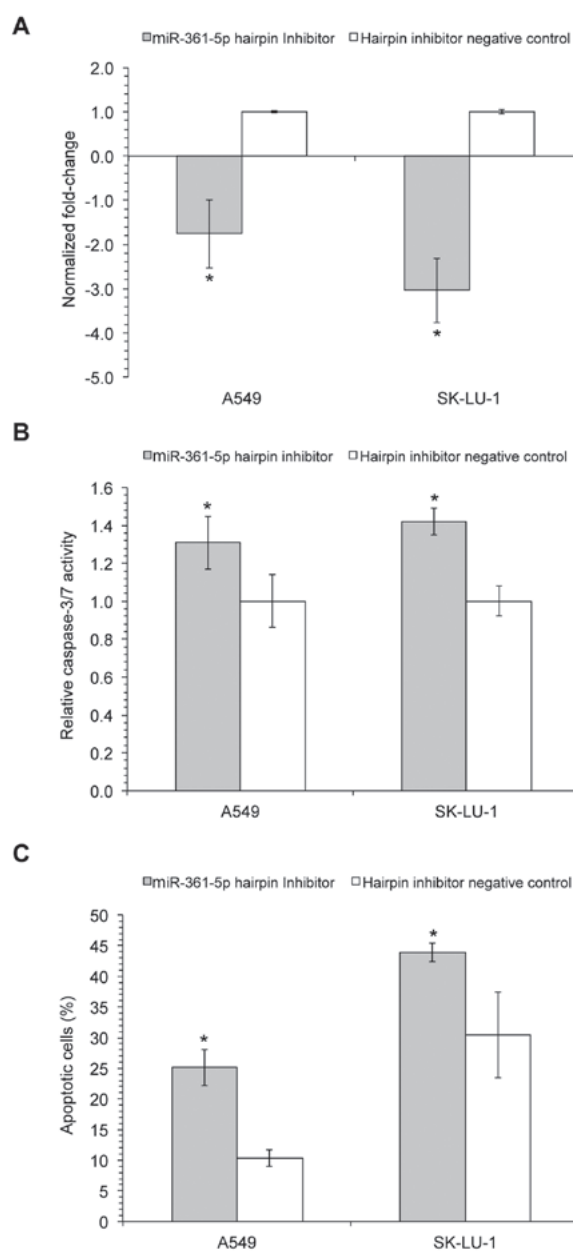

Figure 1. The biological effects of miR-361-5p on the apoptotic properties of A549 and SK-LU-1 cells. (A) Normalized fold change of miR-361-5p hairpin inhibitor transfected cells. Samples were normalized to the endogenous control, RNU6. (B) Caspase-3/7 activity detection at 48 h post-transfection. (C) Detection of apoptosis at 72 h post-transfection using flow cytometry after Annexin V-FITC/PI staining. Data are presented as the means ± SD from 3 biological replicates. *P<0.05, statistically significant difference vs. hairpin inhibitor negative control group.

lung adenocarcinoma cell lines. The silencing of *Bcl-xL* in the A549 cells has been shown to downregulate miR-361-5p expression (7). In this study, to investigate the biological effects of miR-361-5p, miR-361-5p hairpin inhibitor and hairpin inhibitor negative control were transiently transfected into the lung adenocarcinoma cells, A549 and SK-LU-1. The results from RT-qPCR indicated that the transfection of miR-361-5p hairpin inhibitor successfully suppressed miR-361-5p expression levels, when compared to the hairpin inhibitor negative control (Fig. 1A), whereas transfection with miR-361-5p mimics significantly increased
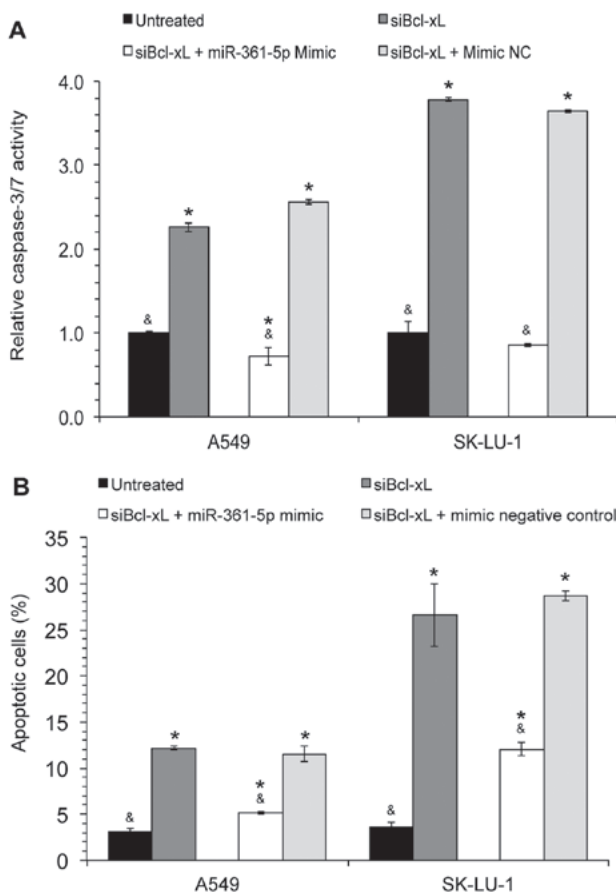
Figure 2. Transfection with miR-361-5p mimics inhibits the si*Bcl-xL*-induced apoptosis of A549 and SK-LU-1 cells. (A) Caspase-3/7 activity at 48 h post-transfection. (B) Detection of apoptosis at 72 h post-transfection using flow cytometry after Annexin V-FITC/PI staining. Data are presented as the means ± SD from 3 biological replicates. *P<0.05, statistically significant difference vs. untreated group; &P<0.05, statistically significant difference vs. si*Bcl-xL* + miR-361-5p mimic NC group.
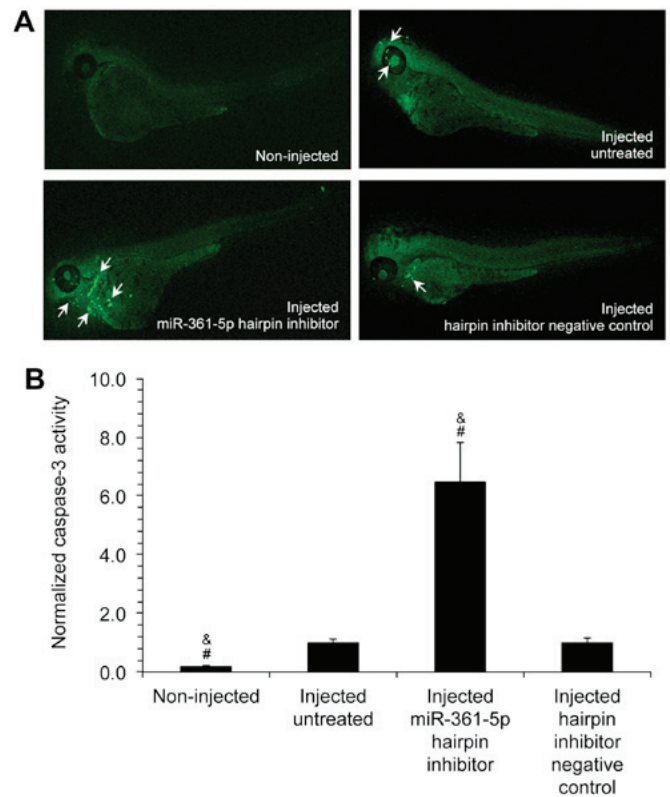

Figure 3. Inhibition of miR-361-5p induces caspase-3 activation *in vivo*. (A) Representative images of zebrafish embryos examined by confocal microscopy following the injection of cells transfected with the miR-361-5p hairpin inhibitor. Arrows indicate positive active caspase-3 staining. (B) Fluorescence was quantified and analyzed using ImageJ Analyst software to generate normalized arbitrary fluorescence units. Data are presented as the means ± SD from 15 biological replicates. #P<0.05, statistically significant difference vs. hairpin inhibitor negative control group; &P<0.05, statistically significant difference vs. injected untreated group.

miR-361-5p expression (data not shown). Furthermore, the inhibition of miR-361-5p expression resulted in a significant increase in caspase-3/7 activities in both the A549 and SK-LU-1 cells (1.31±0.14 and 1.42±0.07 relative activity, respectively; Fig. 1B). Correspondingly, the detection of cell death at 72 h post-transfection, using flow cytometry after Annexin V-FITC/PI staining, indicated that the inhibition of miR-361-5p resulted in a significant increase in the percentage of apoptotic A549 and SK-LU-1 cells (25.10±2.94 and 43.93±1.53%, respectively) in comparison to the hairpin inhibitor negative control (Fig. 1C). However, no significant change in apoptosis and caspase activity was observed when miR-361-5p was overexpressed using mimics (data not shown).

Transfection with miR-361-5p mimics blocks siBcl-xL-induced cell death. To elucidate the association between *Bcl-xL*, miR-361-5p and apoptosis, a combination study was performed whereby the cells were first transfected with si*Bcl-xL* followed by transfection with miR-361-5p mimics. The data revealed that the relative caspase-3/7 activity in the *Bcl-xL*-silenced cells was significantly decreased following miR-361-5p mimic transfection (Fig. 2A); a similar decrease in the percentage of apoptotic A549 and SK-LU-1 cells was observed (Fig. 2B),

thus demonstrating that the overexpression of miR-361-5p was able to block si*Bcl-xL*-induced cell death.

Transfection with miR-361-5p inhibitors increases caspase-3 expression in zebrafish embryo animal models. To analyze the *in vivo* effects of miR-361-5p on apoptosis, zebrafish were used as an animal model. A549 cells transfected with either miR-361-5p inhibitor or hairpin inhibitor negative controls were microinjected into zebrafish embryos. Following staining with anti-rabbit fluorophore-conjugated antibodies, the embryos were visualized using a Leica confocal microscope (Fig. 3A). The analysis of the fluorescent images using ImageJ software indicated that th caspase-3 levels were significantly increased by 6.41±1.04-fold in the embryos injected with miR-361-5p hairpin inhibitor-transfected cells in comparison to the embryos injected with hairpin inhibitor negative control-transfected cells (Fig. 3B). These results suggested that the downregulation of miR-361-5p expression was also able to induce apoptosis *in vivo*.

miR-361-5p is predicted to bind to SMAD2 3'UTR. To elucidate the underlying molecular mechanisms responsible for miR-361-5p-mediated apoptosis, an in silico approach was used to identify the putative target genes of miR-361-5p using the TargetScan database, followed by gene-annotation
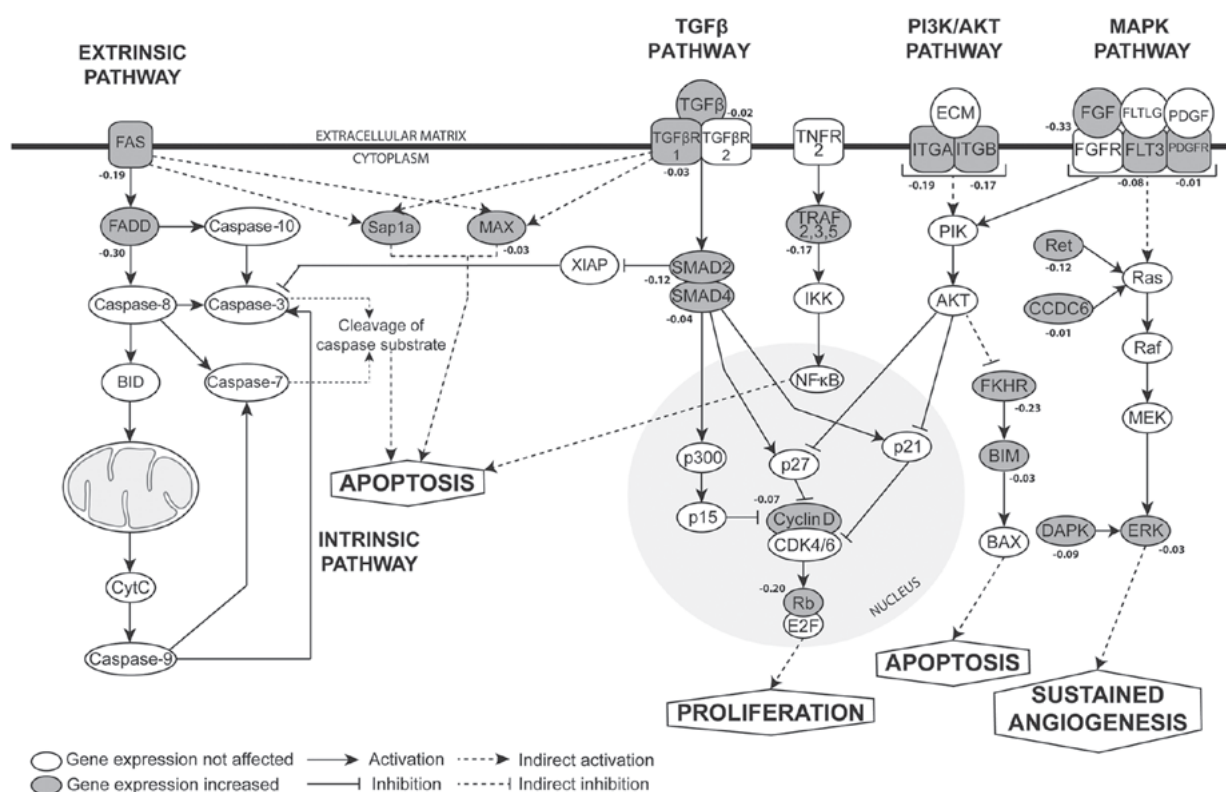
Figure 4. A hypothetical signaling network showing the interaction of downregulated miR-361-5p and its putative targets in various biological pathways. Key signaling pathways of apoptosis regulation were predicted to include the transforming growth factor β (TGFβ), phosphatidylinositol 3-kinase/protein kinase B (PI3K/AKT), mitogen activated protein kinase (MAPK) and the intrinsic and extrinsic pathway. Genes in grey indicate those predicted to be targeted by miR-361-5p. Numbers indicate total context+ score for that specific target with miR-361-5p.

enrichment analyses using the web tool, DAVID, which categorizes the predicted miR-361-5p targets into apoptosis-related pathways. The enrichment of genes involved in cancer pathways indicated the possible involvement of the transforming growth factor β (TGFβ), phosphatidylinositol 3-kinase/protein kinase B (PI3K/AKT) pathway and mitogen-activated protein kinase (MAPK) pathways, together with the intrinsic and extrinsic apoptotic pathways as potential targets of miR-361-5p (Fig. 4). SMAD2, a cytoplasmic signaling protein, was identified as a predicted target of miR-361-5p, with a total context+ score of -0.12.

miR-361-5p directly binds to the SMAD2 3'UTR, decreasing its protein expression. Among the various target genes, *SMAD2* was selected for further experimental validation as it contains two seed-recognizing miR-361-5p binding sites and is known to be involved in apoptosis and proliferation (20-22). The *SMAD2* 3'UTR and its corresponding mutant counterpart, were cloned into the 3' end of the pmirGLO Dual-Luciferase miRNA Target Expression Vector (Fig. 5A). Relative Firefly luciferase activity, measured in the presence of miR-361-5p mimic/inhibitors or their respective negative controls were measured. The results indicated that the cells co-transfected with wild-type constructs (WT 3'UTR) and miR-361-5p mimics exhibited a substantial 0.35-fold decrease in relative luciferase activity in comparison to the cells in the control group (Fig. 5B). In the cells co-transfected with the mutant constructs (Mut 3'UTR), no significant differences were observed between the relative luciferase activities. This

observation indicates that miR-361-5p can directly bind to the binding sequence on the 3'UTR of *SMAD2*, suppressing its gene expression; this was further verified by a decrease in SMAD2 protein levels as determined by western blot analysis (Fig. 5C and D).

The ectopic overexpression of SMAD2, without the 3'UTR, restores the effects of miR-361-5p on the A549 and SK-LU-1 lung adenocarcinoma cell lines. The results of this study indicated that miR-361-5p suppresses the apoptosis of A549 and SK-LU-1 cells, and inhibits SMAD2 expression. Therefore, it was predicted that the miR-361-5p-mediated inhibition of apoptosis may in part be attributed to the function of SMAD2. To confirm that the effects of miR-361-5p on apoptosis are mediated by *SMAD2*, gene rescue experiments were performed, whereby a *SMAD2* expression vector (pCMV6/SMAD2, lacking its 3'UTR) was co-transfected into the A549 and SK-LU-1 cells along with the miR-361-5p mimic. The SMAD2 protein expression levels were measured at 48 h post transfection and it was found that transfection with pCMV6/SMAD2 'rescued' or reversed the decrease in protein expression that was observed in the cells transfected only with miR-361-5p mimics (Fig. 6A and B). Furthermore, transfection with pCMV6/SMAD2 was able to partially reverse the inhibition of apoptosis induced by miR-361-5p (Fig. 6C and D). Taken together, these observations suggest that the oncogenic role of miR-361-5p in lung adenocarcinoma cells is at least partially due to the inhibition of its target gene, *SMAD2*.
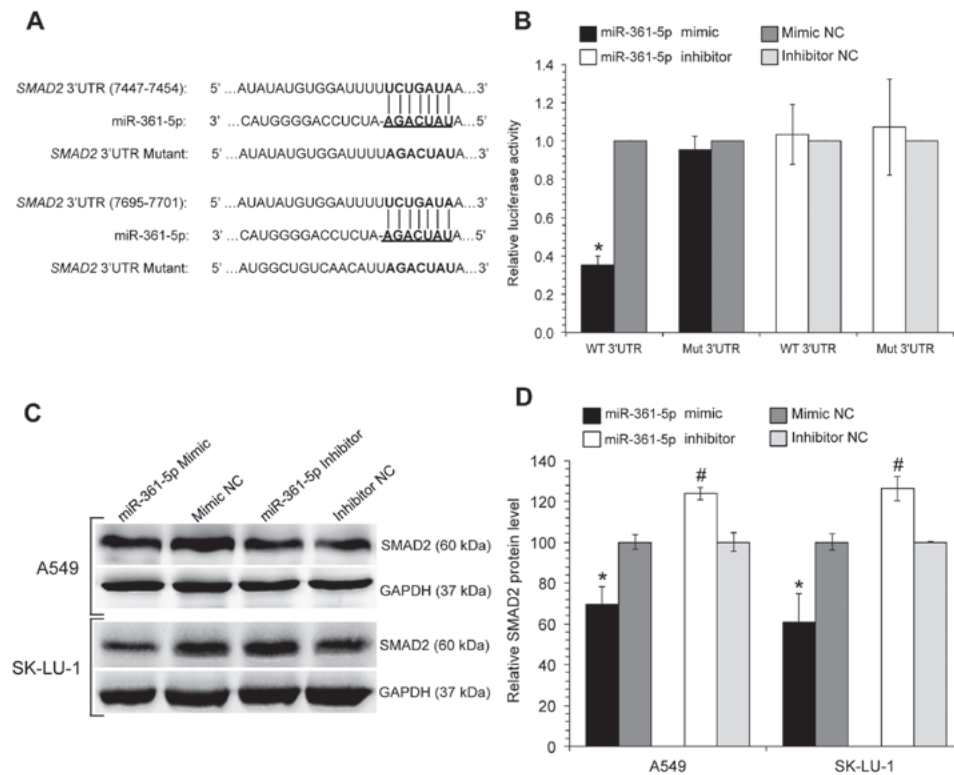
Figure 5. miR-361-5p directly targets *SMAD2*. (A) Sequence alignment of miR-361-5p and *SMAD2* 3'UTR. *SMAD2* 3'UTR contains two predicted miR-361-5p binding sites. (B) Normalized relative luciferase activity in wild-type (WT 3'UTR) and mutant (Mut 3'UTR) pmirGLO/SMAD2 constructs in response to transfection of A549 cells with miR-361-5p mimic or mimic NC and miR-361-5p inhibitor or inhibitor NC. Samples were normalized to *Renilla* luciferase activity. (C) Western blot analysis of SMAD2 protein following miR-361-5p transfection. (D)The intensities of the proteins were quantified using the ImageJ Analyst software and results were standardized against the levels of GAPDH and presented as relative expression. Data are presented as mean ± SD from 3 biological replicates. *P<0.05, statistically significant difference vs. mimic NC group; #P<0.05, statistically significant difference vs. inhibitor NC group. Mimic NC and inhibitor NC were used as negative controls.
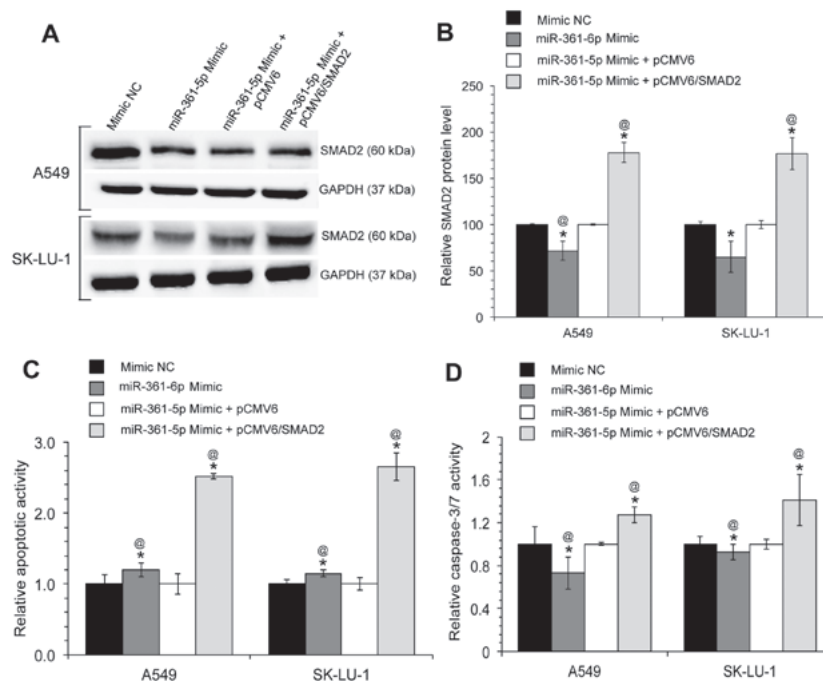

Figure 6. Ectopic overexpression of *SMAD2*, without 3'UTR, restores the miR-361-5p-induced effects on non-small cell lung cancer cells. (A) Western blot analysis of SMAD2 protein expression following co-transfection with miR-361-5p mimics and pCMV6/SMAD2. (B) The intensities of the proteins were quantified using ImageJ Analyst software. The results were standardized against the levels of GAPDH and are presented as relative expression. (C) Detection of the apoptosis of A549 and SK-LU-1 at 48 h post co-transfection with miR-361-5p mimics and pCMV6/SMAD2 vectors. (D) Detection of caspase-3/7 activity in A549 and SK-LU-1 at 48 h post co-transfection with miR-361-5p mimics and pCMV6/SMAD2 vectors. Data are presented as the means ± SD from 3 biological replicates. *P<0.05, statistically significant difference vs. mimic NC group; @P<0.05, statistically significant difference vs. miR-361-5p Mimic + pCMV6 group. pCMV6 denotes empty vectors. pCMV6/SMAD2 denotes *SMAD2* overexpression vector. Mimic NC and empty pCMV6 vectors were used as negative controls.

Discussion

The anti-apoptotic *Bcl-xL* protein is frequently found to be overexpressed in lung adenocarcinoma, playing an important role in the inhibition of apoptosis, and is therefore a critical contributor to tumor development and progression (23). Our previous study demonstrated that the silencing of *Bcl-xL* triggers alterations in the miRNA expression profiles of A549 lung adenocarcinoma cells and the rippling effects of these miRNA expression alterations towards target genes may contribute to the inducement of apoptosis (7). miR-361-5p was one of the miRNAs found to be significantly downregulated following *Bcl-xL* silencing, and the present study aimed to determine the role of miR-361-5p in the apoptotic properties of *Bcl-xL*-silenced human lung adenocarcinoma cells.

Previous studies have demonstrated that in different cancer types, miR-361-5p can function as either a tumor suppressive or an oncogenic miRNA (oncomiR). For example, in colorectal and gastric cancer, miR-361-5p has been shown to act as a tumor suppressor, and to inhibit cancer cell proliferation, invasion and metastasis by directly binding and decreasing the expression of staphylococcal nuclease domain containing-1 (SND1) (24). miR-361-5p also functions as a tumor suppressor in castration-resistant prostate cancer (25) and hepatocellular carcinoma (26) by suppressing cell proliferation and triggering apoptosis, through the direct inhibition of signal transducer and activator of transcription 6 (STAT6) and C-X-C chemokine receptor type 6 (CXCR6), respectively. Furthermore, an increased expression of miR-361-5p has reported to be associated with a better prognosis in patients with breast cancer (27). Conversely, miR-361-5p functions as an oncomiR in cervical cancer, enhancing the promotion of growth and increasing the migration/invasion capacity of cells through mediation of epithelial-to-mesenchymal (EMT) transition (28).

The results of this study indicated that the inhibition of miR-361-5p expression led to an increase of the apoptosis of A549 and SK-LU-1 cells *in vitro* and *in vivo*. Furthermore, co-transfection experiments demonstrated that miR-361-5p overexpression was able to block the apoptosis induced by the silencing of *Bcl-xL*. These results suggest that miR-361-5p plays an oncogenic role in the regulation of apoptosis in NSCLC. The reasons that miR-361-5p plays differential roles in various cancer types is not yet well understood; however, it is suggested that the specific functions of miR-361-5p may be tissue- or cell-specific and may strongly be dependent upon their downstream targets. Further studies are warranted to elucidate the role of miR-361-5p in different cell lines and types of cancer.

In this study, to identify the cellular target through which miR-361-5p regulates apoptosis, bioinformatics analysis revealed that two regions in the *SMAD2* 3'UTR mRNA have perfect complementary binding sites to the seed sequence of miR-361-5p. Luciferase activity assays indicated that miR-361-5p binds to the 3'UTR sequence of *SMAD2* mRNA, confirming that *SMAD2* is a direct target of miR-361-5p. Given that miR-361-5p was downregulated in *Bcl-xL*-silenced A549 cells (7) and that it negatively regulates *SMAD2* expression, we hypothesized that the targeting of *SMAD2* may be a mechanism through which miR-361-5p acts as an oncomiR in NSCLC.

SMADS are a family of structurally related proteins that function as signal transducers of TGFβ family member proteins and play an important role in regulating cell growth inhibition, cellular senescence, differentiation and apoptosis (29-33). SMAD2, a receptor-regulated SMAD (R-Smads), has been proposed to be a tumor suppressor and the decreased expression of SMAD2 has been observed in human cancers (34-37). Emerging evidence has demonstrated the critical role of SMAD2 in apoptosis. For example, Yang *et al* (38) provided one of the first studies on SMAD2 functioning as a tumor suppressor and identified SMAD2 as a critical mediator of the TGFβ-induced apoptosis of prostate epithelial cells. In another study, Yang *et al* also demonstrated that SMAD2 together with Rb/E2F4, the cell cycle-regulated repressor element (CDE) and the cell cycle gene homology region (CHR), were able to suppress the expression of *survivin*, an inhibitor of apoptosis, and to induce the apoptosis of prostate epithelial cells (20). SMAD2 has also been shown to activate the DAP-kinase promoter, thus associating SMAD2 with mitochondrial-based pro-apoptotic events (32). Furthermore, various studies have indicated that SMAD2 can downregulate the X-linked inhibitor of apoptosis protein (XIAP), inducing caspase-3 activation and TRAIL-induced apoptosis (39-41).

In conclusion, the findings of the present study demonstrated that miR-361-5p acts as an oncogenic miRNA in NSCLC and that the downregulation of this miRNA induces apoptosis *in vitro* and *in vivo*. Its role as an oncogenic miRNA was attributed towards the direct targeting of *SMAD2*, a novel gene target. Notably, gene rescue experiments demonstrated that the miR-361-5p-mediated inhibition of the apoptosis of A549 and SK-LU-1 cells was reversed by the re-introduction of the SMAD2 protein. These results indicate that the downregulation of *SMAD2* by miR-361-5p is likely to be an authentic mechanism of miR-361-5p-mediated oncogenesis in NSCLC, thus suggesting that the inhibition of miR-361-5p may be a promising therapeutic strategy for NSCLC.

Availability of data and materials

The datasets used and/or analyzed during the current study are available from the corresponding author on reasonable request.

Authors' contributions

NO and NHN conceived and designed the experiments; NO performed the experiments; NO and NHN analyzed the data; NO and NHN wrote the manuscript.

Ethics approval and consent to participate

Approval was obtained from the University of Malaya, Faculty of Medicine, Institutional Care of Use Committee (FOM IACUC) (Ethics reference no. 2015-181006/IBS/R/NO) and complied with all relevant animal welfare laws, guidelines and policies.

Patient consent for publication

Not applicable.

Competing interests

The authors declare that they have no competing interests.

References

1. Ferlay J, Soerjomataram I, Ervik M, Forman D, Bray F, Dikshit R, Elser S, Mathers C, Rebelo M and Parkin DM: GLOBOCAN 2012 v1.0, Lung Cancer. Estimated Incidence, Mortality and Prevalence Worldwide in 2012. International Agency for Research on Cancer. World Health Organization, Lyon, 2013. http://globocan.iarc.fr/Pages/fact_sheets_cancer.aspx. Accessed July 7, 2017.
2. Pfister DG, Johnson DH, Azzoli CG, Sause W, Smith TJ, Baker S Jr, Olak J, Stover D, Strawn JR, Turrisi AT, et al; American Society of Clinical Oncology: American Society of Clinical Oncology treatment of unresectable non-small-cell lung cancer guideline: Update 2003. J Clin Oncol 22: 330-353, 2004.
3. Howlader N, Noone A, Krapcho M, Miller D, Bishop K, Altekruse SF, Kosary CL, Yu M, Ruhl J, Tatalovich Z, et al: SEER Cancer Statistics Review, 1975-2013. National Cancer Institute, Bethesda, MD, 2017. https://seer.cancer.gov/archive/csr/1975_2013/. Accessed July 7, 2017.
4. Sorenson CM: Bcl-2 family members and disease. Biochim Biophys Acta 1644: 169-177, 2004.
5. Liam CK, Pang YK, Leow CH, Poosparajah S and Menon A: Changes in the distribution of lung cancer cell types and patient demography in a developing multiracial Asian country: Experience of a university teaching hospital. Lung Cancer 53: 23-30, 2006.
6. Soini Y, Kinnula V, Kaarteenaho-Wiik R, Kurttila E, Linnainmaa K and Pääkkö P: Apoptosis and expression of apoptosis regulating proteins bcl-2, mcl-1, bcl-X, and bax in malignant mesothelioma. Clin Cancer Res 5: 3508-3515, 1999.
7. Othman N, In LL, Harikrishna JA and Hasima N: Bcl-xL silencing induces alterations in hsa-miR-608 expression and subsequent cell death in A549 and SK-LU1 human lung adenocarcinoma cells. PLoS One 8: e81735, 2013.
8. Bartel DP: MicroRNAs: Genomics, biogenesis, mechanism, and function. Cell 116: 281-297, 2004.
9. Hayashita Y, Osada H, Tatematsu Y, Yamada H, Yanagisawa K, Tomida S, Yatabe Y, Kawahara K, Sekido Y and Takahashi T: A polycistronic microRNA cluster, miR-17-92, is overexpressed in human lung cancers and enhances cell proliferation. Cancer Res 65: 9628-9632, 2005.
10. Shivdasani RA: MicroRNAs: Regulators of gene expression and cell differentiation. Blood 108: 3646-3653, 2006.
11. Phuah NH, Azmi MN, Awang K and Nagoor NH: Down-regulation of microRNA-210 confers sensitivity towards 1'S-1'-acetoxychavicol acetate (ACA) in cervical cancer cells by targeting SMAD4. Mol Cells 40: 291-298, 2017.
12. Mott JL, Kobayashi S, Bronk SF and Gores GJ: mir-29 regulates Mcl-1 protein expression and apoptosis. Oncogene 26: 6133-6140, 2007.
13. Othman N and Nagoor NH: The role of microRNAs in the regulation of apoptosis in lung cancer and its application in cancer treatment. BioMed Res Int 2014: 318030, 2014.
14. Koo KH and Kwon H: MicroRNA miR-4779 suppresses tumor growth by inducing apoptosis and cell cycle arrest through direct targeting of PAK2 and CCND3. Cell Death Dis 9: 77-91, 2018.
15. Yuan L, Li S, Zhou Q, Wang D, Zou D, Shu J and Huang Y: miR-124 inhibits invasion and induces apoptosis of ovarian cancer cells by targeting programmed cell death 6. Oncol Lett 14: 7311-7317, 2017.
16. Lv KT, Liu Z, Feng J, Zhao W, Hao T, Ding WY, Chu JP and Gao LJ: miR-22-3p regulates cell proliferation and inhibits cell apoptosis through targeting the eIF4EBP3 gene in human cervical squamous carcinoma cells. Int J Med Sci 15: 142-152, 2018.
17. Gang L, Qun L, Liu WD, Li YS, Xu YZ and Yuan DT: MicroRNA-34a promotes cell cycle arrest and apoptosis and suppresses cell adhesion by targeting DUSP1 in osteosarcoma. Am J Transl Res 9: 5388-5399, 2017.
18. Grimson A, Farh KK, Johnston WK, Garrett-Engele P, Lim LP and Bartel DP: MicroRNA targeting specificity in mammals: Determinants beyond seed pairing. Mol Cell 27: 91-105, 2007.
19. Huang W, Sherman BT and Lempicki RA: Systematic and integrative analysis of large gene lists using DAVID bioinformatics resources. Nat Protoc 4: 44-57, 2009.
20. Yang J, Song K, Krebs TL, Jackson MW and Danielpour D: Rb/E2F4 and Smad2/3 link survivin to TGF-beta-induced apoptosis and tumor progression. Oncogene 27: 5326-5338, 2008.
21. Jang CW, Chen CH, Chen CC, Chen JY, Su YH and Chen RH: TGF-beta induces apoptosis through Smad-mediated expression of DAP-kinase. Nat Cell Biol 4: 51-58, 2002.
22. Van Themsche C, Chaudhry P, Leblanc V, Parent S and Asselin E: XIAP gene expression and function is regulated by autocrine and paracrine TGF-beta signaling. Mol Cancer 9: 216-228, 2010.
23. Leech SH, Olie RA, Gautschi O, Simões-Wüst AP, Tschopp S, Häner R, Hall J, Stahel RA and Zangemeister-Wittke U: Induction of apoptosis in lung-cancer cells following bcl-xL antisense treatment. Int J Cancer 86: 570-576, 2000.
24. Ma F, Song H, Guo B, Zhang Y, Zheng Y, Lin C, Wu Y, Guan G, Sha R, Zhou Q, et al: miR-361-5p inhibits colorectal and gastric cancer growth and metastasis by targeting staphylococcal nuclease domain containing-1. Oncotarget 6: 17404-17416, 2015.
25. Liu D, Tao T, Xu B, Chen S, Liu C, Zhang L, Lu K, Huang Y, Jiang L, Zhang X, et al: miR-361-5p acts as a tumor suppressor in prostate cancer by targeting signal transducer and activator of transcription-6 (STAT6). Biochem Biophys Res Commun 445: 151-156, 2014.
26. Sun JJ, Chen GY and Xie ZT: MicroRNA-361-5p inhibits cancer cell growth by targeting CXCR6 in hepatocellular carcinoma. Cell Physiol Biochem 38: 777-785, 2016.
27. Cao ZG, Huang YN, Yao L, Liu YR, Hu X, Hou YF and Shao ZM: Positive expression of miR-361-5p indicates better prognosis for breast cancer patients. J Thorac Dis 8: 1772-1779, 2016.
28. Wu X, Xi X, Yan Q, Zhang Z, Cai B, Lu W and Wan X: MicroRNA-361-5p facilitates cervical cancer progression through mediation of epithelial-to-mesenchymal transition. Med Oncol 30: 751-762, 2013.
29. Derynck R, Zhang Y and Feng XH: Smads: Transcriptional activators of TGF-beta responses. Cell 95: 737-740, 1998.
30. Itoh S, Itoh F, Goumans MJ and Ten Dijke P: Signaling of transforming growth factor-beta family members through Smad proteins. Eur J Biochem 267: 6954-6967, 2000.
31. Massagué J: How cells read TGF-beta signals. Nat Rev Mol Cell Biol 1: 169-178, 2000.
32. Massagué J and Wotton D: Transcriptional control by the TGF-beta/Smad signaling system. EMBO J 19: 1745-1754, 2000.
33. Miyazono K: TGF-beta signaling by Smad proteins. Cytokine Growth Factor Rev 11: 15-22, 2000.
34. Hoot KE, Lighthall J, Han G, Lu SL, Li A, Ju W, Kulesz-Martin M, Bottinger E and Wang XJ: Keratinocyte-specific Smad2 ablation results in increased epithelial-mesenchymal transition during skin cancer formation and progression. J Clin Invest 118: 2722-2732, 2008.
35. Munker S, Weng HL, Li Q, Liu Y, Meyer C, Dooley S and Li J: Differential Smad expression contributes to severity of cholangiocarcinoma. Z Gastroenterol 50: K102, 2012.
36. Wu Y, Li Q, Zhou X, Yu J, Mu Y, Munker S, Xu C, Shen Z, Müllenbach R, Liu Y, et al: Decreased levels of active SMAD2 correlate with poor prognosis in gastric cancer. PLoS One 7: e35684, 2012.

37. Samanta D and Datta PK: Alterations in the Smad pathway in human cancers. Front Biosci 17: 1281-1293, 2012.
38. Yang J, Wahdan-Alaswad R and Danielpour D: Critical role of Smad2 in tumor suppression and transforming growth factor-beta-induced apoptosis of prostate epithelial cells. Cancer Res 69: 2185-2190, 2009.
39. Wang H, Jiang JY, Zhu C, Peng C and Tsang BK: Role and regulation of nodal/activin receptor-like kinase 7 signaling pathway in the control of ovarian follicular atresia. Mol Endocrinol 20: 2469-2482, 2006.
40. Xu G, Zhou H, Wang Q, Auersperg N and Peng C: Activin receptor-like kinase 7 induces apoptosis through up-regulation of Bax and down-regulation of Xiap in normal and malignant ovarian epithelial cell lines. Mol Cancer Res 4: 235-246, 2006.
41. Xu F, Zhou D, Meng X, Wang X, Liu C, Huang C, Li J and Zhang L: Smad2 increases the apoptosis of activated human hepatic stellate cells induced by TRAIL. Int Immunopharmacol 32: 76-86, 2016.